



OPEN Metabolomics reveal taste quality differences of black teas and the impact of withering on quality formation

Juan Yang, Shanmin Chen, Jie Wang, Yulai Zhang, Rui Chang, Ying Zhang, Hongyu Luo & Linying Yuan

Taste is one of the important factors for evaluating the quality of tea. Smart tongue and metabolomics were used to analyze the difference in taste of Gongou black teas from three different varieties. In this study, 564 non-volatile metabolites (NVMs) were identified in the black teas. The quality difference between Shuyong 3 black tea (SY-T) and Fuding Dabai black tea was the greatest, followed by SY-T and Sichuan Small and Medium-leaf black tea. Specially, the differential NVMs primarily influenced the astringency, sourness, umami, and bitterness taste attributes of black teas, rather than sweetness. Based on the correlation results between differential NVMs and the taste of black tea, and in combination with the VIP value ≥ 1.5 , 24 characteristic differential NVMs that might have a significant impact on the formation of different taste qualities were successfully screened out. In the withering process, the differential metabolic pathways of three different varieties were primarily concentrated in flavonoid and carbohydrate metabolic pathways, which was potentially explaining the main cause of alterations in the characteristic metabolites and the taste profiles of the black teas. Our findings provide a theoretical basis for the taste variations among different varieties, as well as a new insights into the quality formation of black tea during the withering process.

Keywords Gongou black tea, Taste, Variety, Withering process, Metabolic pathway

Black tea, is the most produced and consumed tea globally. It is widely favored for its distinctive “red leaves and red liquor” quality and its various health benefits^{1,2}. Congou black tea, as a unique type of Chinese black tea, has its quality primarily influenced by tea cultivars³, natural environment⁴, and processing techniques^{5,6}. The various flavors⁷ of Congou black tea from different origins aptly meet consumers’ diverse preferences. Chongqing Congou black tea is produced from fresh leaves of tea cultivars predominantly grown in Chongqing region. Fresh leaves undergo processing steps including withering, fermentation, and drying. It is characterized by a dark, glossy appearance, a bright red liquor, a rich sweet aroma, and a robust, refreshing taste. Notably, teas made from different cultivars have significant variations in quality^{8,9}, exhibiting distinct regional identity of Chongqing Congou black tea.

Withering is the first crucial step in shaping black tea quality^{5,10}. Recent research indicates that moderately reducing leaf moisture content (30–40%) during withering significantly enhances the visual appearance and polyphenol conversion rate^{11,12}. Dehydration stress triggers chemical reactions among non-volatile compounds within the tea leaves^{13,14}, leading to a decrease in astringent and bitter catechins and flavonoid glycosides, while promoting the accumulation of sweet-tasting amino acids such as theanine and glutamate. These changes collectively contribute to the distinctive sensory profile and biochemical signature of black tea^{15,16}. Indeed, the alterations in non-volatile metabolites during processing work as a fundamental prerequisite for the formation of its unique flavor.

Among the assessments of tea quality, taste is a crucial parameter and the key determinant of market value¹⁷. Extensive studies have demonstrated that the sensory characteristics of tea liquor are closely linked to its key chemical components, including tea polyphenols, amino acids, and soluble sugars¹⁸. However, these sensory properties are not only determined by these components, but more precisely by their specific types, relative concentrations, and their interactions^{19,20}. The metabolomic mechanisms underlying the taste variations among different Congou black teas remain largely unexplored. Understanding how withering, as the initial processing

Tea Research Institute, Chongqing Academy of Agricultural Sciences, Yongchuan, Chongqing 402160, China.
 email: 350129893@qq.com

stage, modulates the metabolic network to influence substance transformation in subsequent stages, and thereby ultimately shapes the taste profiles of Congou black teas, holds considerable theoretical and practical importance for optimizing black tea processing techniques and enhancing overall tea quality.

Therefore, this study employs a widely targeted metabolomics approach based on Ultra Performance Liquid Chromatography-Electrospray Ionization-Tandem Mass Spectrometry (UPLC-ESI-MS/MS), combined with sensory evaluation, to systematically compare the metabolic profiles of Congou black tea produced from three representative tea cultivars in the Chongqing region. We aim to elucidate characteristic metabolic markers associated with taste quality, and to investigate the dynamic changes and regulatory mechanisms of these key metabolites during the withering process. This work is expected to provide novel scientific insights into the material basis underlying taste variations in black tea and the impact of withering on quality formation.

Materials and methods

Reagents and instruments

Methanol, acetonitrile and ammonium acetate were all of the chromatographic purity and purchased from Merck (Darmstadt, Hesse, Germany). Formic acid was purchased from TCI (Shanghai) Development Co., Ltd. (Shanghai Chemical Industry Park, China). The standards of (+)-catechin (C), (-)-gallocatechin (GC), (-)-epicatechin (EC), (-)-epicatechin gallate (ECG), (-)-epigallocatechin (EGC), (-)-epi-gallocatechin gallate (EGCG), gallic acid (GA) and caffeine (CAF) were all purchased from Sigma-Aldrich (Shanghai, China). High Performance Liquid Chromatography (Agilent 1200) and Agilent Eclipse XD 8 C18 column (250 mm × 4.6 mm i.d., 5 μm) were all from Agilent Technologies (Santa Clara, CA, USA). Ultra-high performance liquid chromatography (Acquity I-Class PLUS) was from Waters Corp. (Milford, MA, USA). Mass spectrometer (AB Sciex Qtrap 6500+) was from SCIEX (Framingham, MA, USA). Chromatographic column (Acquity UPLC HSS T3 1.8 μm, 2.1 mm × 100 mm) was from Waters Corp. (Milford, MA, USA). 4-16KS high-speed centrifuge was from Sigma-Aldrich Corp. (St. Louis, MO, USA). SpectraMax 190 multi-wavelength microplate reader was from MD Corp. (San Jose, CA, USA).

Sample preparation

All raw materials (*Camellia sinensis* (L.) O. Kuntze) consisting of one bud with one leaf or two leaves were harvested from the same batch of fresh tea leaves of three varieties respectively named “Fuding Dabai” (FD), “Sichuan small and medium leaf” (SM) and “Shuyong 3” (SY) in the tea garden of Chongqing Academy of Agricultural Sciences (Yongchuan, Chongqing, China). The collection of plants material complies with relevant institutional, national and international guidelines and legislation. And permission for the collection of the plant material was obtained by the Chongqing Academy of Agricultural Sciences. The plant materials were authenticated by Associate Researcher Xiumin Zhai from Chongqing Academy of Agricultural Sciences.

The fresh leaves were immediately transported to a withering environment at a temperature of 26 ± 2 °C and relative humidity (RH) $76 \pm 2\%$. Following a period of 0, 4, 8, 12 and 16 h of withering, the second leaf below bud of withered tea leaves were gathered and promptly treated with liquid nitrogen, five withering samples were collected and named W0, W4, W8, W12, W16, respectively. After withering, samples were then subjected to the traditional manufacturing process of rolling (100 ~ 120 min), oxidation (28 ± 2 °C, RH $95 \pm 2\%$) and drying (100 ± 5 °C, 30 min), resulting in the production of Congou black tea samples. Finally, three tea samples were obtained and named SM-T, FD-T and SY-T. Each sample was created with three independent duplicates and thereafter kept at -80 °C for further analysis. The ultra low temperature freezer which stored the specimens were in the sample storage room of the Chongqing Academy of Agricultural Sciences at 20 ± 5 °C, 55–75% relative humidity.

Electronic tongue analysis

The electronic tongue sensor was activated and preheated with 15 mL 0.01 mol/L potassium chloride solution, and then tested alternately with cleaning solution (ultra-pure water) and standard product. The signal value was appropriate between 0.5 and 10 V, and six parallel repetitions were taken. After the standard test, the sensor is optimized and the original signal value is analyzed by partial least square (PLS) to establish the model. After the PLS model was established and optimized successfully, the samples were tested (the brewing method was consistent with the sensory review), and the concentrations of each taste attribute were predicted with 3 times of parallelism.

Sensory evaluation

The sensory evaluation of the tea beverages was conducted by a team of five trained members consisting of three males and two females from the Tea Research Institute, Chongqing Academy of Agricultural Sciences. All team members were certified by the Ministry of Human Resources and Social Security, the People's Republic of China for their expertise in tea quality evaluation. The evaluation process followed the guidelines set by the national standard for tea (GB/T 23,776–2018)²¹. The sensory evaluation encompassed the assessment of sensory factors related to appearance, color, aroma, taste, and infused leaf. Besides, the taste was evaluated by employing the equivalent quantification method (on a 10-point scale) to score the intensity of bitterness, astringency, sweetness, sourness, and umami in the tea infusion²². The intensity values of taste attributes were scored using a scale from 0 to 10 (0–2 represents extremely weak, 2–4 represents weak, 5–6 represents moderate, 7–8 represents strong and 9–10 represents extremely strong). Tea infusions were blind-evaluated using random codes. Each sample was evaluated three times. Above all, the sensory evaluation in this study was executed in accordance with relevant guidelines and regulations, all experimental protocols have been approved by designated institutions and licensing committees, and informed consent had been obtained from all tasters.

Tea polyphenols, water extract, free amino acids, catechins and caffeine analysis

The contents of total tea polyphenols, water extract and free amino acids were detected by GB/T 8313–2008²³, GB/T 8305–2013²⁴ and GB/T 8314–2013²⁵, respectively. The contents of individual catechins and caffeine were determined according to HPLC²⁶. Tea infusions preparation: added 5 mL 70% methanol (preheated in 70 °C water bath) to 0.2 g tea sample, incubated at 70 °C water bath for 10 min, centrifuged at 1 200 g for 10 min after cool down, transferred the supernatant to a 10 mL volumetric flask; repeated the above steps, combined the supernatant, then diluted to 10 mL as mother tea liquid; diluted 2 mL of mother tea liquid to 10 mL with distilled water as final tea liquid, passed through 0.45 µm organic membrane for testing. The injected sample volume was 5 µL with flow rate of 0.9 mL/min. The UV detection wavelength was set at 278 nm. Individual amino acids were determined by comparing their elution time with standards, and quantitated according to the regression equation of the corresponding calibration curve.

Widely targeted metabolomics analysis

The tea samples were vacuum freeze-dried and randomly selected from each portion for the detection of metabolites. 50 mg of these samples were weighed into eppendorf (EP) tube, followed by adding 1 mL extraction solution (acetonitrile: methanol: water, 2: 2: 1, v/v/v). After vortexing for 30 s, these samples were homogenized at 45 Hz for 10 min and sonicated for 10 min in an ice-water bath. Then, the mixture were stored at –20 °C for 1 h and centrifuged at 12,000 rpm for 15 min at 4 °C. Next, 500 µL of supernatant was transferred to a fresh tube and dried in a vacuum concentrator at 37 °C. The dried samples were reconstituted in 160 µL of 50% acetonitrile, vortexed, sonicated and centrifuged as previously described. Finally, 120 µL of supernatant was transferred to a 2 mL injection bottle for LC–MS analysis. 10 µL of each sample was taken and mixed as quality control (QC) samples.

The extracts were analyzed using an UPLC–ESI–MS/MS system (UPLC, Waters Acquity I-Class PLUS; MS, Applied Biosystems QTRAP 6500+). The analytical conditions were as follows, UPLC: column, Waters HSS-T3 (1.8 µm, 2.1 mm × 100 mm); The mobile phase was consisted of solvent A, pure water with 0.1% formic acid and 5 mM Ammonium acetate, and solvent B, acetonitrile with 0.1% formic acid. Sample measurements were performed with a gradient program that employed the starting conditions of 98% A, 2% B and kept for 1.5 min. Within 5.0 min, a linear gradient to 50% A, 50% B was programmed, Within 9.0 min, a linear gradient to 2% A, 98% B was programmed, and a composition of 2% A, 98% B was kept for 1 min. Subsequently, a composition of 98% A, 2% B was adjusted within 1 min and kept for 3 min. Flow velocity: 0.35 mL/min; column temperature: 50 °C. Injection volume: 2 µL.

The ESI source operation parameters were as follows: source temperature 550 °C; ion spray voltage (IS) 5500 V (positive ion mode)/–4500 V (negative ion mode); ion source gas I (GSI), gas II (GSII), curtain gas (CUR) were set at 50, 55, and 35 psi, respectively; the collision-activated dissociation (CAD) was medium. Instrument tuning and mass calibration were performed with 10 and 100 µmol/L polypropylene glycol solutions in QQQ and LIT modes, respectively. QQQ scans were acquired as MRM experiments with collision gas (nitrogen) set to medium. DP (declustering potential) and CE (collision energy) for individual MRM transitions was done with further DP and CE optimization. A specific set of MRM transitions were monitored for each period according to the metabolites eluted within this period.

Based on the self-built database GB-PLANT, substance identification was conducted according to secondary mass spectrum information. During the analysis, isotope signals, duplicate signals from ions containing K⁺, Na⁺, or NH₄⁺, as well as duplicate signals from fragment ions that are actually fragments of larger-molecular-weight substances, were excluded. Metabolite quantification was accomplished through the analysis utilizing the multiple reaction monitoring (MRM) mode of a triple quadrupole mass spectrometer. In the MRM mode, the first quadrupole initially screened the precursor ions (parent ions) of the target substances, eliminating ions corresponding to substances with other molecular weights to preliminarily reduce interference. After the precursor ions had undergone induced ionization and fragmentation in the collision cell, numerous fragment ions were generated. These fragment ions then passed through the triple quadrupole, where a specific characteristic fragment ion was filtered and selected, further excluding interference from non-target ions and enhancing the accuracy and repeatability of quantification. After the mass spectrometry analysis data of metabolites from different samples had been obtained, peak area integration was performed on the mass spectrometry peaks of all substances. Subsequently, integral correction was carried out on the mass spectrometry peaks of the same metabolite in different samples.

Data analysis

Unsupervised principal component analysis (PCA), orthogonal partial least squares discriminant analysis (OPLS-DA), volcano plots of differential metabolites, dynamic distribution plots, and heatmaps were analyzed and plotted using tools on the Metware cloud platform (<https://cloud.metware.cn>). The filtering criteria for metabolite differences between two groups were: VIP value > 1, *p* value < 0.05, and fold change > 2 or < 0.5. For KEGG functional annotation and pathway enrichment analysis of differential metabolites, as well as correlation heatmaps, data analysis and plotting were carried out using tools on the BMK cloud platform (www.biocloud.net). Other data analysis and plotting were performed using IBM SPSS Statistics 27, Graphpad Prism 19 and Adobe Photoshop 2022.

Results and discussion

Sensory characteristics of Gongou black teas from different varieties

The Congou black teas made from different varieties were evaluated using the sensory evaluation method. There were obvious differences in the appearance and sensory experience among the black teas of the three varieties (Fig. 1a and Table S1). Among them, SY-T exhibits a strong and rich taste profile, while FD-T presents a mellow and

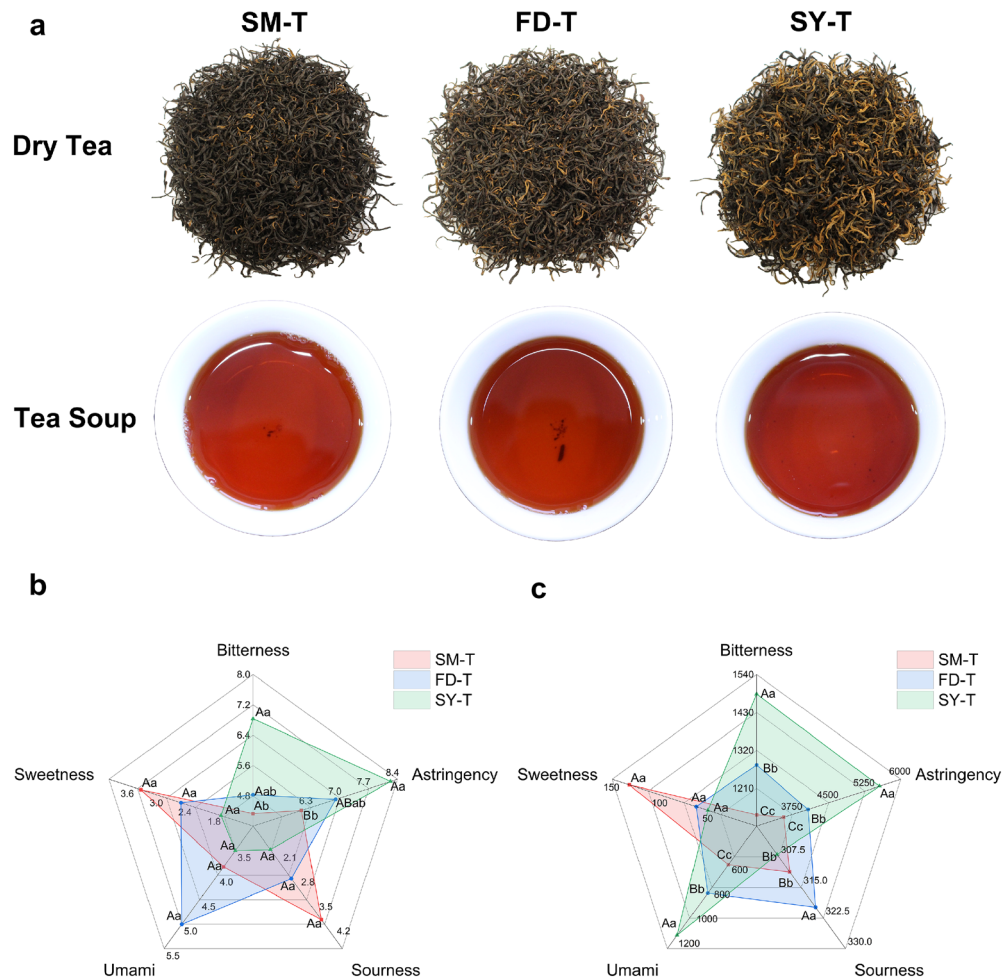


Fig. 1. Characteristics (a) and sensory evaluation (b, c) of Gongou black teas from different varieties. (a): The dry tea and tea infusions of Gongou black teas; (b): The taste sensory evaluation of Gongou black teas by human senses. (c): Electronic tongue prediction of taste intensity in black tea infusions ($\mu\text{g/ml}$). The different uppercase/lowercase letters indicate the least significant difference ($p < 0.01/0.05$).

refreshing taste, and SM-T demonstrates a mellow and rich taste. In sensory evaluation of taste profiles (Fig. 1b), it was observed that the three Congou black teas exhibited consistent trends in bitterness and astringency. SY-T demonstrated the highest intensity for both bitterness and astringency, followed by FD-T. Significant differences in bitterness were found among the three varieties ($p < 0.01$), while astringency showed notable variation only between SY-T and SM-T ($p < 0.01$). Conversely, sourness and sweetness displayed inverse trends compared to bitterness and astringency, with SM-T showing a stronger intensity, though no significant differences in sensory scores were detected among the varieties ($p > 0.05$). Umami intensity was highest in FD-T, followed by SM-T, but these differences were non-significant ($p > 0.05$). Regarding electronic tongue predictions of taste concentration (Fig. 1c), the order for bitterness, astringency, and umami was SY-T > FD-T > SM-T, with highly significant differences among all three varieties ($p < 0.01$). Sourness concentration followed FD-T > SM-T > SY-T, with FD-T showing significantly higher levels than the others ($p < 0.01$). Sweetness concentration ranked SM-T > FD-T > SY-T, though without significant inter-variety differences ($p > 0.05$). Combining sensory evaluation and electronic tongue predictions, the Congou black teas demonstrated prominent bitterness and astringency, with consistent results between both methods for bitterness, astringency, and sweetness. While discrepancies arose in sourness and umami assessments, the sensory evaluations failed to reach statistical significance, thereby validating the feasibility of electronic tongue-based taste concentration predictions.

Analysis of the main components in Gongou black teas of different varieties

Biochemical constituents constitute the material foundation for the formation of tea's taste quality. It is widely acknowledged that polyphenols primarily contribute to the bitter and astringent flavors^{27,28}, whereas amino acids and soluble sugars are the principal sources of umami and sweetness^{19,29}, respectively. SY-T exhibited a relatively high content of tea polyphenols, which was significantly higher than that in SM-T and FD-T (Fig. 2a). Regarding amino acids, SM-T had the highest content, showing a highly significant difference compared to FD-T and SY-T. Additionally, highly significant variations were observed in the soluble sugar content among the three black teas. FD-T exhibited the highest soluble sugar content, which aligned with the sweet taste profile detected by the

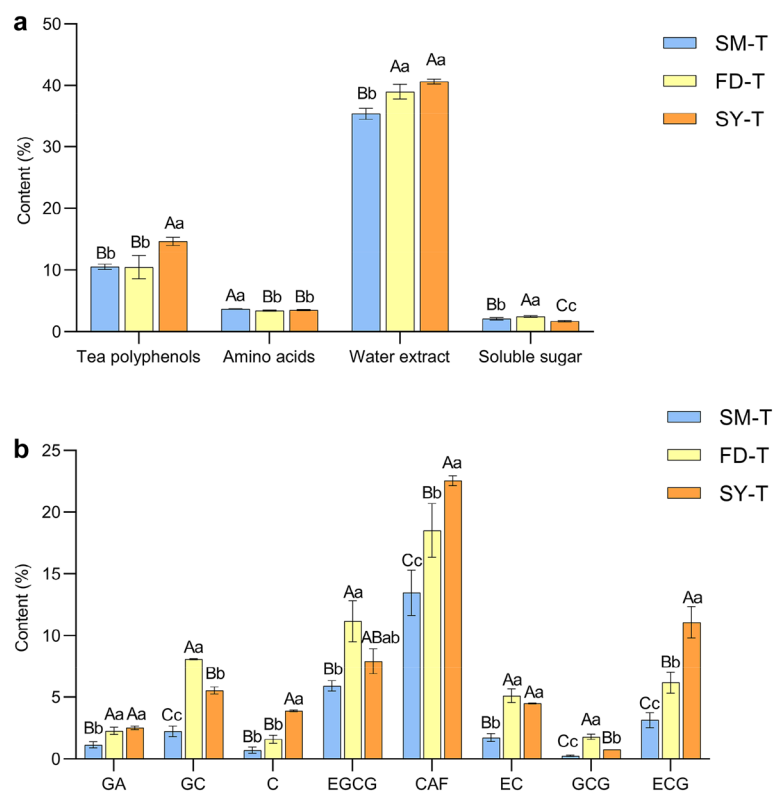


Fig. 2. The main components in Gongou black teas of different varieties. **(a):** The content of the main components; **(b):** The content of the GA, GC, C, EGCG, CAF, EC, GCG, ECG. The different uppercase/lowercase letters indicate the least significant difference ($p < 0.01/0.05$).

electronic tongue, followed by SM-T. The water extract content serves as an indicator of the substance richness in the tea infusion. It was evident that SY-T had the highest water extract content, followed by FD-T, with no statistically significant difference between them. In contrast, SM-T had the lowest water extract content, which was consistent with the sensory evaluation results. Caffeine is recognized as a crucial substance that contributes to the bitter taste of tea and also induces a sense of excitement in individuals^{30,31}. Highly significant differences were observed in the caffeine content among the three tea varieties. Specifically, SY-T exhibited the highest caffeine content, followed by FD-T, while SM-T had the lowest content (Fig. 2b). Catechins represent a class of compounds in tea that impart bitterness and astringency. Additionally, some of these catechins contribute to the sweet aftertaste³². In this study, FD-T was found to be rich in EGCG, GCG, GC, and EC, whereas SY-T contained high levels of ECG, C, and GA (Fig. 2b). In contrast, the contents of these components in SM-T were relatively low.

Analysis of NVMs in Gongou black teas of different varieties

Profiles of NVMs in Gongou black teas of different varieties

Through wide-targeted metabolomics determination, a total of 564 non-volatile metabolites (NVMs) were identified in the black teas of the three varieties. Specifically, there were 553 NVMs in SM-T, 546 in FD-T, and 542 in SY-T, with 524 metabolites commonly present in the samples (Fig. 3a). The compositions of NVMs in each variety were largely similar, encompassing a total of 19 types of primary metabolites. The primary metabolites with relatively high proportions were as follows: flavonoids accounted for 19.0–19.7%, terpenoids for 10.4–10.5%, sugars and alcohols for 10.3–10.5%, amino acids for 9.2–9.6%, and organic acids for 8.3–8.5% (Fig. 3b). Notably, the number of flavonoid types in SM-T (109 types) was 6 more than that in FD-T and 4 more than that in SY-T, respectively.

Screening of differential NVMs in Gongou black teas of different varieties

Principal Component Analysis (PCA) and Orthogonal Projections to Latent Structures Discriminant Analysis (OPLS—DA) were employed to identify NVMs in black teas of different varieties. The results indicated that there were significant overall differences among the samples (Fig. 3c). The R^2Y and Q^2 values of the OPLS—DA evaluation models reached 0.997 and 0.949, respectively. Differential metabolites were screened according to the significant difference criteria, namely $VIP > 1$, $p < 0.05$, and $FC \geq 2$ or $FC \leq 1/2$ (Fig. 3d). Specifically, 114 differential NVMs were identified in the comparison of FD-T vs SY-T, 66 in SM-T vs FD-T, and 88 in SM-T vs SY-T. Additionally, 199 differential NVMs were identified in the comparison among SM-T, FD-T, and SY-T (Fig. 3e). Based on these findings, it was speculated that there might be a relatively large quality gap between SY-T and FD-T, followed by that between SM-T and SY-T. Among the 199 differential NVMs, the primary

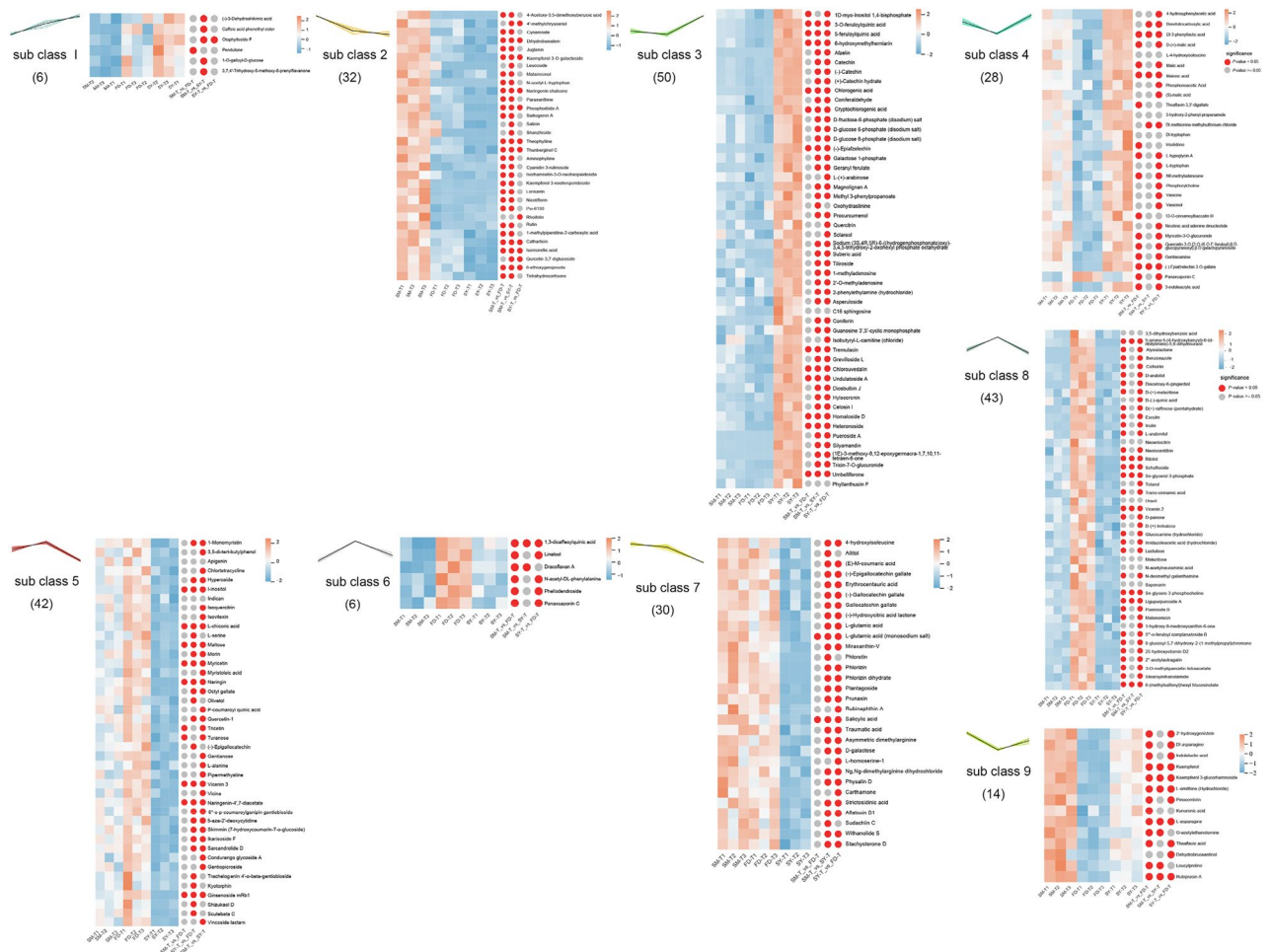


Fig. 4. Clusters and heat map of differential NVMs in black teas of different varieties.

In Cluster 2, differential NVMs, such as Dihydrobaicalein, Kaempferol-3-O-Galactoside, Naringenin Chalcone, Pheophorbide A, Theophylline, and Thunberginol C, demonstrated relatively elevated concentrations in SM-T. Similarly, in Cluster 7, L-Glutamic Acid (Monosodium Salt) and Salicylic Acid, as well as in Cluster 9, Kaempferol, Kaempferol 3-Glucorhamnoside, L-Ornithine (Hydrochloride), L-Asparagine, and Rubiprasin A, also exhibited notably high levels in SM-T. Furthermore, the concentrations of these differential NVMs in SM-T were significantly distinct from those in the other two varieties.

In Cluster 6, differential NVMs including I-Inositol, L-Chicoric Acid, Maltose, Myricetin, Naringin, Vicenin 3, Naringenin-4',7'-diacetate, and Ginsenoside mRb1 exhibited relatively elevated concentrations in FD-T. Similarly, 1,3-Dicaffeoylquinic Acid in Cluster 5, as well as 5-Amino-5-(4-Hydroxybenzyl)-6-(D-Ribitylimino)-5,6-Dihydrouracil, Ribitol, Schaftoside, Sn- Glycerol 3-Phosphate, Vicenin 2, Sn-Glycero-3-Phosphocholine, Ligupurpuroside A, and 6-(Methylsulfonyl)Hexyl Glucosinolate in Cluster 8, also demonstrated notably high levels in FD-T. Furthermore, the concentrations of these differential NVMs in FD-T were significantly distinct compared to those in the other two varieties.

In Cluster 3, differential NVMs including 3-O-Feruloylquinic Acid, 5-Feruloylquinic Acid, 6-Hydroxymethylherniarin, Chlorogenic Acid, Cryptochlorogenic Acid, (-)-Epiafzelechin, Tremulacin, Chlorouvedalin, and Undulatoside A, as well as those in Cluster 4, namely DI-3- Phenyllactic Acid, Malonic Acid, and (-)-Epiafzelechin 3-O-gallate, exhibited notably elevated concentrations in SY-T. Furthermore, the concentrations of these differential NVMs in SY-T were significantly distinct compared to those in the other two varieties. In summary, the aforementioned metabolites may serve as the characteristic differential NVMs of black teas from different varieties.

Correlation analysis of main components, differential NVMs and taste in Black Teas of different varieties

As depicted in Fig. 5a, in the black teas of three varieties, no statistically significant correlation was observed between free amino acids, ECCG, GC, and the taste attributes of black tea. Conversely, tea polyphenols, water extracts, CAF, ECG, GA, and C exhibited significant to highly significant correlations with bitterness, astringency, and umami. Soluble sugar and GCG demonstrated a significant positive correlation with sourness,

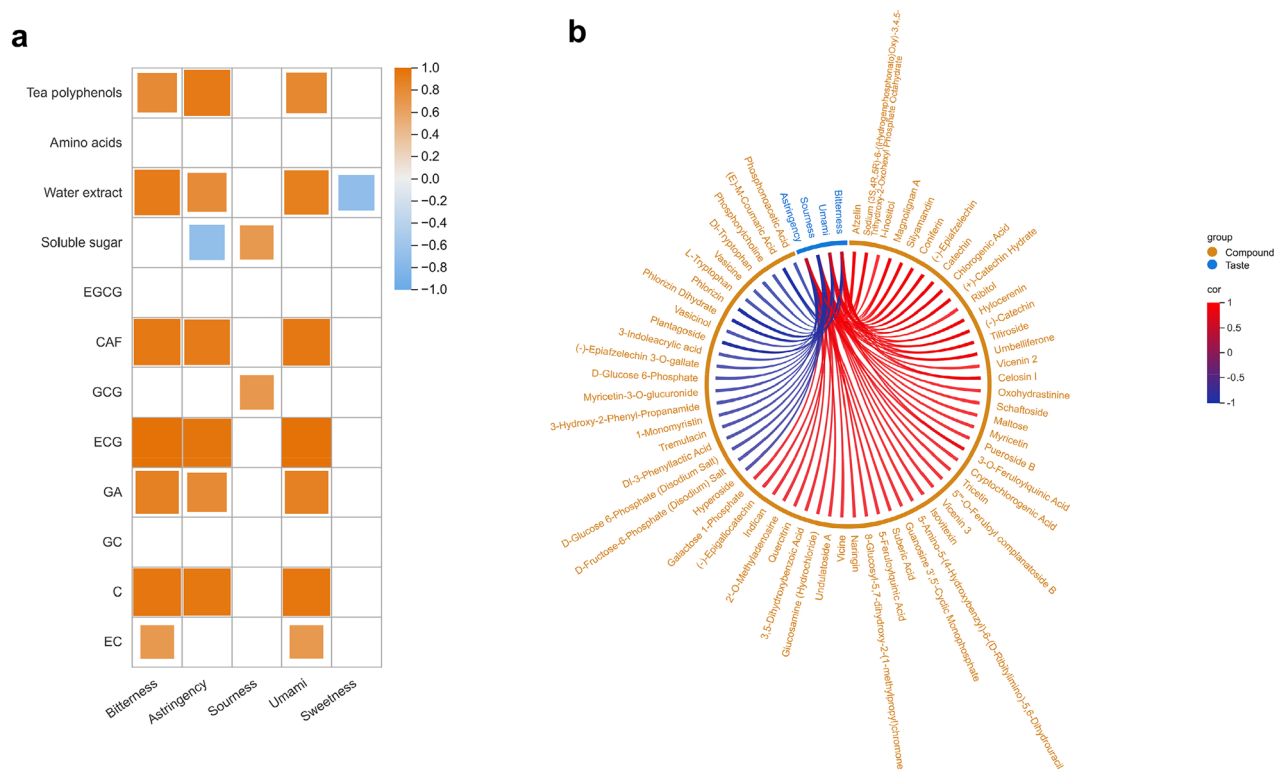


Fig. 5. Correlation between main components, differential NVMs and the taste of black teas of different varieties. **(a):** Heat map of the correlation between main components and the taste of black teas. **(b):** Circular graph of the correlation between differential NVMs and the taste of black teas.

while EC showed a significant positive correlation with both bitterness and umami. Notably, only water extracts were negatively correlated with sweetness, and soluble sugar was negatively correlated with astringency.

As illustrated in Fig. 5b and Table S2, the differential NVMs predominantly influenced the taste attributes of black tea, including astringency, sourness, umami, and bitterness. Notably, a total of 34 metabolites displayed a highly significant correlation with sourness, representing the largest number among all taste-related correlations. There were 11 metabolites that exhibited a highly significant correlation solely with astringency. Only one metabolite demonstrated a combined correlation with both umami and astringency. Additionally, 18 metabolites were simultaneously correlated with bitterness, astringency, and umami.

Among these, the metabolites showing a highly significant correlation with sourness mainly originated from flavonoids, alkaloids, organic acids, and sugars and alcohols. Representative metabolites with a positive correlation encompassed (–)-Epigallocatechin, L-Inositol, Schaftoside, etc., while those with a negative correlation encompassed Vasicinol, L-Tryptophan, Phosphorylcholine, etc.

The representative metabolites with a highly significant positive correlation only with astringency were Phosphorylcholine, Suberic Acid, Guanosine 3',5'-Cyclic Monophosphate, etc., and those with a negative correlation were Hyperoside and 1-Monomyristin. The only substance that showed a highly significant correlation with both astringency and umami was 3-O-Feruloylquinic Acid.

Metabolites with a highly significant correlation with bitterness, astringency and umami mainly derived from flavonoids. Representative metabolites with a positive correlation included Chlorogenic Acid, Catechin, (–)-Catechin, etc., and those with a negative correlation were (E)-M-Coumaric Acid, Plantagoside, Phlorizin Dihydrate, and Phlorizin.

Analysis of characteristic differential NVMs in black teas of different varieties

Based on the correlation results between differential NVMs and the taste of black tea, combined with a variable importance in the projection (VIP) value ≥ 1.5 , 24 characteristic differential NVMs were screened out (Table S4). Their contents in black teas of various varieties were presented in Fig. 6. Judging from the original response values of NVMs, among flavonoids, Schaftoside, Vicenin 2, Tricetin, Pueroside B, Isovitecin, Myricetin, and Vicenin 3 were found to be abundant in the FD-T, followed by the SM-T. In contrast, (–)-Epigallocatechin 3-O-gallate, Silyamandin, (+)-Catechin Hydrate, Catechin, and (–)-Catechin were predominantly present in the SY-T, with the SM-T ranking second. Regarding other metabolites, Tremulacin, 3-O-Feruloylquinic Acid, 5-Feruloylquinic Acid, Chlorogenic Acid, Undulatoside A, Cryptochlorogenic Acid, D-Glucose 6-Phosphate, Umbelliferone, and Celosin I were abundant in the SY-T, followed by the SM-T. Conversely, L-Inositol, Ribitol, and Maltose were mainly detected in the FD-T, with the SM-T ranking second. In summary, the characteristic

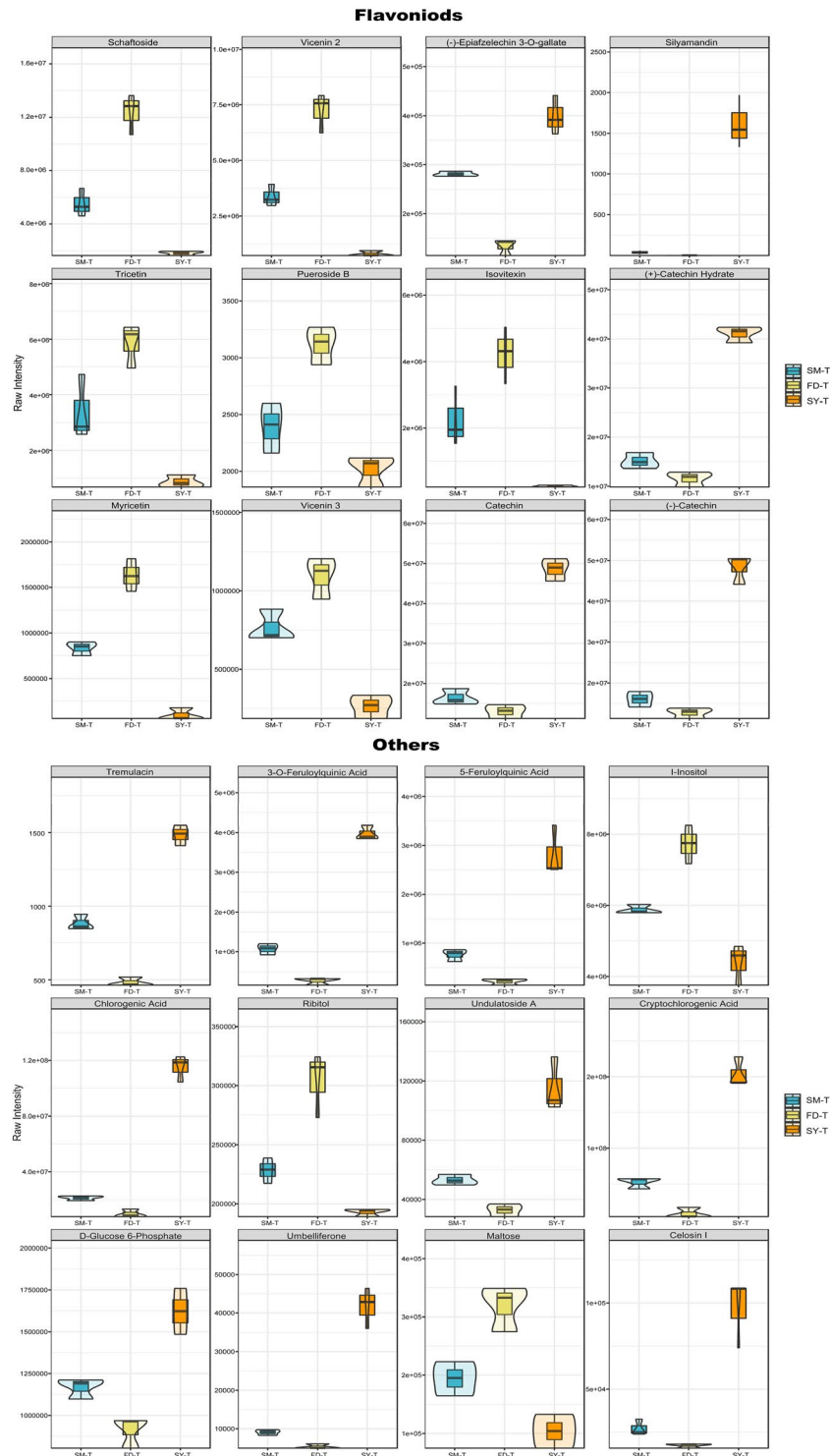


Fig. 6. Violin plot of characteristic differential NVMs in black teas of different varieties.

differential NVMs of the FD-T were mostly flavonoids, whereas the SY-T exhibited a more diverse range of characteristic differential NVMs.

Influence of withering on the changes of taste compounds in black teas

Dynamic changes of NVMs during the withering process

The K-means clustering analysis method was also employed to cluster the NVMs in the withered leaves of three varieties. The NVMs from the withering process of the FD variety were successfully grouped into three clusters. In contrast, those from the withering processes of the SM and SY varieties were respectively clustered into

four clusters, and these clusters exhibited different changing trends (Fig. 7). Specifically, regarding the changing trends of metabolites in the FD variety (Fig. 7a), the metabolites in Cluster 1 demonstrated a continuous upward trend from 0 to 8 h of withering, followed by a steep decline from 8 to 12 h, and then a slow increase from 12 to 16 h. Cluster 2 showed a continuous upward trend throughout the withering process. Meanwhile, Cluster 3 exhibited a continuous downward trend, with a relatively slow decline rate from 4 to 8 h of withering.

In the SM variety (Fig. 7b), the changing trends of metabolites in Cluster 1 and Cluster 2 were similar to those observed in the FD variety. Specifically, for Cluster 3, the NVMs exhibited a downward trend during the first half of the withering stage, which was largely consistent with the trend in the FD variety. However, the content of these NVMs remained stable in the later stage. The NVMs in Cluster 4 demonstrated a fluctuating trend characterized by an initial increase followed by a decrease. These NVMs were likely to constitute the main material basis for the difference in the taste of black tea between the SM and FD varieties.

The changing trends of NVMs in the SY variety during withering were not entirely consistent with those of the previous two varieties (Fig. 7c). Specifically, the NVMs in Cluster 1 exhibited a step-like downward trend as the withering process progressed. In Cluster 2, the NVMs initially decreased, then increased, and subsequently decreased again, with a relatively significant increase during the 8–12 h withering stage. Given that the changing patterns of these NVMs differed from those in the previous two varieties, it was hypothesized that they might be the characteristic differential metabolites of the SY variety. Cluster 3 demonstrated a trend of increasing first and then decreasing. The increase was relatively significant from 0 to 4 h, and the content stabilized after 12 h of withering. In contrast, Cluster 4 showed a continuous upward trend, which was similar to the trend of Cluster 2 in the FD and SM varieties. It was hypothesized that these metabolites might be common to the three varieties and share similar metabolic pathways.

KEGG enrichment analysis of the metabolic pathways of differential NVMs during the withering process

The Kyoto Encyclopedia of Genes and Genomes (KEGG)³⁴ was employed to perform functional annotation and enrichment analysis of the differential NVMs in the withered leaves of the three varieties at each stage. A total of 154 metabolites were annotated from the three varieties. The number of annotated differential NVMs exhibited

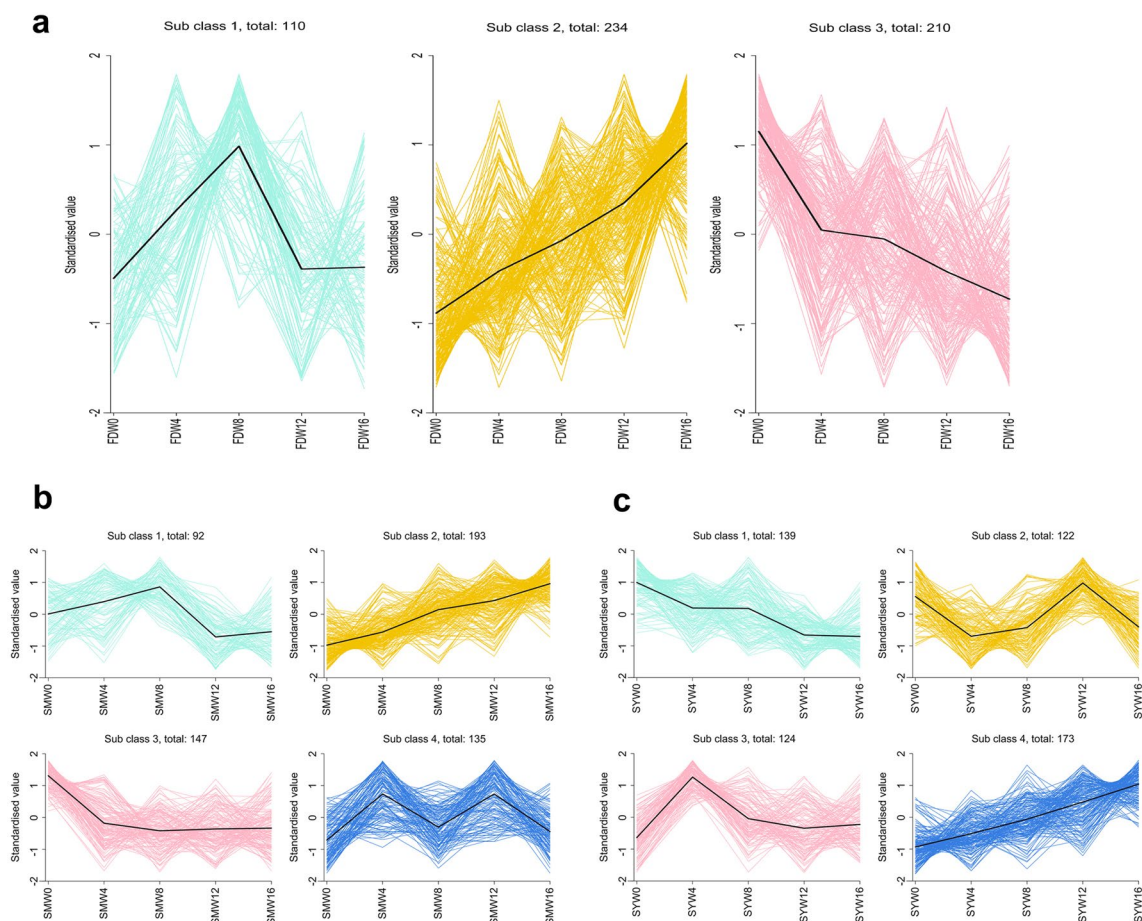


Figure 7 K-means clustering diagram of NVMs during the withering process of different varieties;

Fig. 7. K-means clustering diagram of NVMs during the withering process of different varieties; (a): FD variety; (b): SM variety; (c): SY variety.

variation among different comparison groups during the withering process of different varieties, indicating that the metabolic directions at each stage of withering differed among the varieties.

Specifically, as the withering process progressed, the numbers of annotated differential NVMs in different groups of the SM variety were 13, 13, 7, and 5 in sequence; for the FD variety, the numbers were 17, 8, 6, and 4; and for the SY variety, they were 17, 16, 17, and 11 (Table S3). It can be observed that the NVMs in the SY variety changed substantially during the withering process, with more significant changes occurring in the later stage. In contrast, the NVMs in the FD variety underwent substantial changes in the early stage of withering, while those in the SM variety changed significantly in the middle stage. The top 20 pathways with the most significant enrichment in each comparison group were presented as shown in Fig. S1.

During SM variety withering (Fig. S1), in the SMW0 vs SMW4 stage, differential NVMs exhibited relatively high enrichment factors in Aminoacyl-tRNA biosynthesis, Glucosinolate biosynthesis, Arginine and proline metabolism, and Valine, leucine, and isoleucine degradation. Additionally, a substantial number of differential NVMs were enriched in ABC transporters. During the SMW4 vs SMW8 stage, differential NVMs also showed relatively high enrichment factors in Aminoacyl-tRNA biosynthesis, ABC transporters, Glucosinolate biosynthesis, and Valine, leucine, and isoleucine degradation. These enrichment pathways were largely consistent with those in the previous stage, and all demonstrated an up-regulated trend. This suggests that amino acid metabolism dominated the main change process at this stage. In the SMW8 vs SMW12 stage, the largest number of differential NVMs were enriched in Amino sugar and nucleotide sugar metabolism, while Ubiquinone and other terpenoid-quinone biosynthesis had the highest enrichment factor. The NVMs in this pathway exhibited a down-regulated trend. During the SMW12 vs SMW16 stage, differential NVMs had the highest enrichment factor in Sphingolipid metabolism. It was evident that in the later stage of withering, these three pathways (Amino sugar and nucleotide sugar metabolism, Ubiquinone and other terpenoid-quinone biosynthesis, Sphingolipid metabolism) were all related to plant defense and stress adaptation^{35–37}. This indicates that the differential NVMs at this stage mainly originated from metabolic pathways involved in regulating plant defense, stress adaptation, and programmed cell death under stress conditions.

During FD variety withering (Fig. S2), differential NVMs exhibited relatively high enrichment factors in Glycerophospholipid metabolism, D-Amino acid metabolism, and Alanine, aspartate, and glutamate metabolism, with an up-regulated trend in the FDW0 vs FDW4 stage. In the FDW4 vs FDW8 stage, D-Amino acid metabolism, Aminoacyl-tRNA biosynthesis, Glucosinolate biosynthesis, Arginine and proline metabolism, and Alanine, aspartate, and glutamate metabolism showed relatively high enrichment, also demonstrating an up-regulated trend. These enrichment pathways were akin to those during the first half-stage of SM variety withering, suggesting that amino acid metabolism also dominated the main changes at this stage. During the FDW8 vs FDW12 stage, Vitamin B6 metabolism, D-Amino acid metabolism, and Nitrogen metabolism had relatively high enrichment factors, showing an upward regulation trend. Moreover, a substantial number of metabolites were enriched in ABC transporters. In the FDW12 vs FDW16 stage, five metabolic pathways were enriched. Among them, Isoflavonoid biosynthesis had the highest enrichment factor with an upward regulation trend, followed by Tyrosine metabolism, which exhibited a downward regulation trend. This indicates that during the second half-stage of withering, not only were there pronounced changes in amino acids, but also significant alterations in flavonoids and vitamins.

During SY variety withering (Fig. S3), 13 metabolic pathways were enriched in the SYW0 vs SYW4 stage. Among these pathways, Galactose metabolism, Starch and sucrose metabolism, and Pentose and glucuronate interconversions exhibited relatively high enrichment factors with a substantial number of NVMs. Additionally, a large number of metabolites were enriched in ABC transporters, suggesting that carbohydrate metabolism dominated the main changes at this stage. During the SYW4 vs SYW8 stage, metabolic pathways such as D-Amino acid metabolism, Alanine, aspartate, and glutamate metabolism, Cyanoamino acid metabolism, and Aminoacyl-tRNA biosynthesis were enriched, all showing an up-regulated trend. The pathways including D-Amino acid metabolism, Arginine and proline metabolism, and Aminoacyl-tRNA biosynthesis were also enriched in the SYW8 vs SYW12 stage, all demonstrating an up-regulated trend. This indicates that amino acid metabolism dominated the main changes in the above two stages. In the SYW12 vs SYW16 stage, 13 metabolic pathways were enriched. The NVMs had relatively high enrichment factors in pathways such as beta-Alanine metabolism, Betalain biosynthesis, and Fatty acid biosynthesis. This suggests that at this stage, not only were there pronounced changes in amino acids, but also significant alterations in some differential metabolites, such as pigments and fatty acids.

Overall, during the withering process of the three varieties, the metabolic pathways of NVMs displayed both similarities and differences. The similarities were mainly reflected in the fact that the enriched metabolic pathways were predominantly concentrated in amino acid transformation, primarily occurring in the early and middle stages of withering. The differences mainly resided in that different varieties also exhibited enrichment in the metabolism of flavonoids, fatty acids, carbohydrates, etc., and the majority of these enrichments occurred in the later stage of withering. This result partially aligned with previous studies⁸. For the SM variety, the enrichments were mainly focused on Ubiquinone and other terpenoid-quinone biosynthesis as well as Sphingolipid metabolism. The FD variety showed enrichments primarily in Vitamin B6 metabolism and Isoflavonoid biosynthesis. Regarding the SY variety, the enrichments were centered on carbohydrate metabolism in the early stage and Betalain biosynthesis and Fatty acid biosynthesis in the later stage. These metabolic pathways may have been crucial for contributing to the distinct tastes of black teas from different varieties.

Analysis of the influence mechanism of the withering stage on the taste quality formation of Congou black tea

Through a combined analysis of the 24 screened characteristic differential NVMs and the KEGG-enriched metabolic pathways during the withering process (Table S4), it was found that the differential metabolic pathways were primarily concentrated in flavonoid and carbohydrate metabolic pathways (Fig. 8). During withering, the

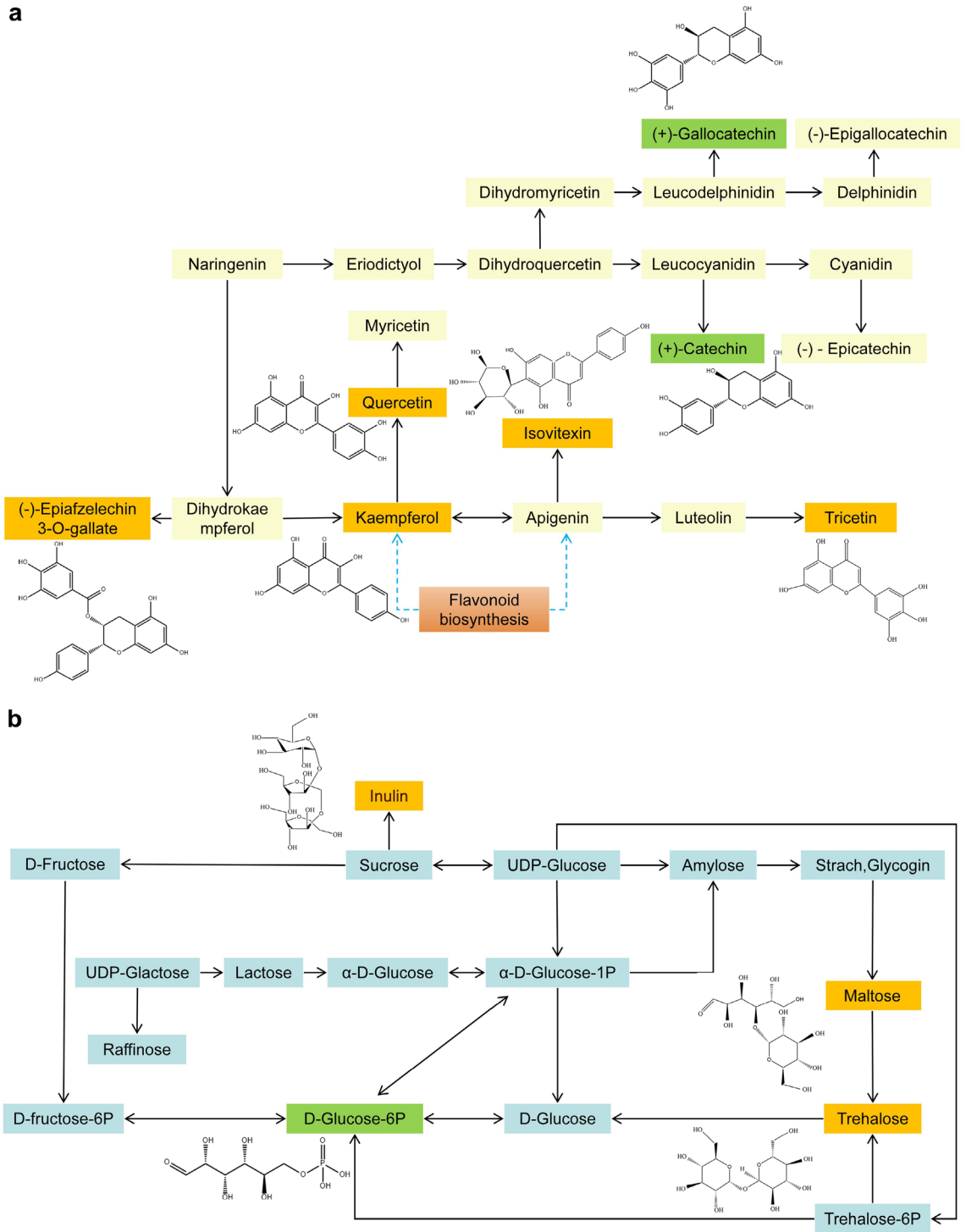


Fig. 8. Metabolic pathway maps of flavonoid (a) and carbohydrate (b) metabolites in the withered process of three black teas. *Note:* Green boxes indicate down regulation of metabolites, while orange boxes indicate up regulation. The blue dashed link points to other metabolic pathways.

anabolic activities of metabolites such as quercetin, kaempferol, (-)-epigallocatechin 3-O-gallate, isovitexin and tricetin were enhanced, leading to a significant downregulation of competing metabolites like (+)-gallocatechin and (+)-catechin. This could be the primary reason for the changes in the flavonoid metabolites and astringent taste profile in black tea infusion. Meanwhile, the upregulated synthesis of metabolites such as sucrose, inulin, maltose and trehalose during withering resulted in a notable decrease of D-glucose-6-phosphate (D-glucose-6P), potentially explaining the main cause of alterations in the characteristic carbohydrate metabolites and the umami taste profiles in black tea infusion.

Conclusion

This study identified the correlations between chemical components and taste attributes in different Congou black teas. The transformation mechanisms and metabolic pathways of these components during the withering process were explored. Distinct taste profiles of black teas from different varieties were identified. Specifically, SY-T exhibited the highest level of bitterness and astringency, characterized by a strong and rich taste profile, while SM-T demonstrated a lower level of mellow taste and is soft and delicate. FD-T, by contrast, displayed intermediate bitterness/astringency, showing a balanced, refreshing aftertaste.

564 types of NVMs were identified through comprehensive targeted metabolomics analysis. Most significant quality disparity was observed between SY-T and FD-T, followed by that between SY-T and SM-T. The diverse tastes of the teas were primarily manifested in terms of bitterness, astringency, umami, and sourness. Twenty-four characteristic differential NVMs, which might impact the distinct taste profiles, have been screened out. There were marked differences in the substance metabolism of black teas from various varieties during withering process. The common metabolic pathway among the three varieties during withering was amino acid transformation, and predominantly occurred in the early and middle stages of withering. Meanwhile, metabolism of flavonoids, fatty acids, and carbohydrates has also been identified, with most of the processes happening in the later stage of withering. Further combined analysis with the screened 24 differential metabolites identified that the differential metabolic pathways were primarily in flavonoid and carbohydrate metabolic pathways. The competitive metabolism of relevant ketone and carbohydrate metabolites was proposed to be the primary factors affecting the taste of different black teas during the withering process.

This study has several limitations. First of all, as our study focuses only on the Congou black tea produced in Chongqing region, the geographical cover and cultivar diversity of the samples are therefore limited. Future research should expand the geographical and cultivar coverage to provide a more comprehensive understanding of the taste variations and their underlying chemical basis in black teas from different areas and varieties. Secondly, while this research primarily investigated the role of withering—a key processing stage—in quality formation, the whole black tea processing chain involves subsequent steps such as rolling, fermentation, and drying. The further transformation of metabolites and their effect on the final taste profile through these later stages have not been explored. Future studies could implement dynamic metabolic tracking throughout the entire processing sequence. Finally, the associations between the characteristic NVMs and sensory attributes are primarily based on statistical analysis. The direct sensory contribution mechanisms, such as interactions between these metabolites and taste receptors, remain to be validated. Follow-up work integrating sensomics and molecular biology approaches is needed for functional verification.

Data availability

All data generated or analysed during this study are included in this article and its Supplementary Information files.

Received: 20 April 2025; Accepted: 4 February 2026

Published online: 10 February 2026

References

1. Yilmaz, Y. Health-promoting effects of black tea: A narrative review of clinical trials. *Int. J. Food Sci.* **2025**, 8560718. <https://doi.org/10.1155/IJFO/8560718> (2025).
2. Lingli, S. et al. Microbial fermentation enhances the effect of black tea on hyperlipidemia by mediating Bile Acid metabolism and remodeling intestinal microbes. *Nutrients* **16**, 998. <https://doi.org/10.3390/NU16070998> (2024).
3. Yunfei, H. et al. Study on dynamic changes in characteristic volatile compounds uncovers aroma development of Hainan Dayezhong (Camellia sinensis var. assamica) black tea. *Food Chem.* **477**, 143578–143578. <https://doi.org/10.1016/j.FOODCHEM.2025.143578> (2025).
4. Fei, Y. et al. Determination of geographical origin of Southern Shaanxi Congou black teas using sensory analysis combined with gas chromatography-ion mobility spectrometry. *Foods* **13**, 3904. <https://doi.org/10.3390/FOODS13233904> (2024).
5. Wenjing, H., Guofu, L., Wei-Wei, D. & Jingming, N. Effects of different withering methods on the taste of Keemun black tea. *LWT* **166**, 113791. <https://doi.org/10.1016/j.LWT.2022.113791> (2022).
6. Kuofei, W. et al. Effect of leaf grade on taste and aroma of shaken Hunan black tea. *Foods* **13**, 42. <https://doi.org/10.3390/FOODS13010042> (2023).
7. Cuinan, Y., Zhihui, W., Hua, P., Wenjin, L. & Puxiang, Y. UPLC–QTOF/MS-based non-targeted metabolomics coupled with the quality component, QDA, to reveal the taste and metabolite characteristics of six types of Congou black tea. *LWT* **185**, 115197. <https://doi.org/10.1016/j.LWT.2023.115197> (2023).
8. Juan, Y. et al. Comparison of the suitability of different tea varieties fresh leaves in summer for the production of Congou black tea. *J. Food Saf. Qual.* **10**, 4242–4248 (2019).
9. Juan, Y. et al. Analysis of Aroma components of congou black tea made of different tea varieties in Chongqing. *J. Southwest Univ* **41**, 21–27. <https://doi.org/10.13718/j.cnki.xdzk.2019.06.004> (2019).
10. Dandan, Q. et al. Effect of withering/spreading on the physical and chemical properties of tea: A review. *Compr. Rev. Food Sci. Food Saf.* **23**, e70010. <https://doi.org/10.1111/1541-4337.70010> (2024).
11. Yulong, Y. et al. Effects of withering on the main physical properties of withered tea leaves and the sensory quality of congou black tea. *J. Texture Stud.* **51**, 542–553. <https://doi.org/10.1111/jtxs.12498> (2020).
12. Huajie, W. et al. Novel insights into the effect of withering degree on Dianhong Congou black tea quality. *Int. J. Food Sci. Technol.* **57**, 3713–3726. <https://doi.org/10.1111/IJFS.15697> (2022).
13. Yu, W. et al. Novel insight into the role of withering process in characteristic flavor formation of teas using transcriptome analysis and metabolite profiling. *Food Chem.* **272**, 313–322. <https://doi.org/10.1016/j.foodchem.2018.08.013> (2019).
14. Bernard, N. et al. Integrated transcriptomic and metabolomic analyses reveal changes in Aroma- and taste-related substances during the withering process of black tea. *Foods* **13**, 3977–3977. <https://doi.org/10.3390/FOODS13233977> (2024).
15. Jingtao, Z. et al. Withering degree affects flavor and biological activity of black tea: A non-targeted metabolomics approach. *LWT* **130**, 109535. <https://doi.org/10.1016/j.lwt.2020.109535> (2020).

16. Junfeng, T. et al. Study of the dynamic changes in the non-volatile chemical constituents of black tea during fermentation processing by a non-targeted metabolomics approach. *Food Res. Int.* **79**, 106–113. <https://doi.org/10.1016/j.foodres.2015.11.018> (2016).
17. Quansheng, C. et al. Application of FT-NIR spectroscopy for simultaneous estimation of taste quality and taste-related compounds content of black tea. *J. Food Sci. Technol.* **55**, 4363–4368. <https://doi.org/10.1007/s13197-018-3353-1> (2018).
18. Xiaochun, W. *Tea biochemistry* 191–194 (Agriculture Press, 2003).
19. Liang, Z., Qingqing, C., Daniel, G., Yongquan, X. & Chitang, H. Association between chemistry and taste of tea: A review. *Trend. Food Sci. Technol.* **101**, 139–149. <https://doi.org/10.1016/j.tifs.2020.05.015> (2020).
20. Yifan, L. et al. Deciphering composition-structure-taste relationship of black tea-infusion via assessments of nanoparticles by centrifugal treatment. *LWT* **222**, 117601–117601. <https://doi.org/10.1016/j.lwt.2025.117601> (2025).
21. Shuying, G. et al. *Methodology of sensory evaluation of tea (GB/T 23776–2018)* (Standards Press of China, Beijing, 2018).
22. Xiangyang, G., Chitang, H., Wilfried, S. & Xiaochun, W. Effect of the roasting degree on flavor quality of large-leaf yellow tea. *Food Chem.* **347**, 129016. <https://doi.org/10.1016/j.foodchem.2021.129016> (2021).
23. Weilong, Z., Jianfeng, X. & Ling, X. *Determination of total polyphenols and catechins content in tea (GB/T 8313–2008)* (Standards Press of China, Beijing, 2008).
24. Weilong, Z., Jianfeng, X., Xiaolei, L., Jing, W. & Haitao, S. *Tea—Determination of water extracts content (GB/T 8305–2013)* (Standards Press of China, Beijing, 2013).
25. Weilong, Z., Jianfeng, X., Xiaolei, L., Jing, W. & Haitao, S. *Tea—Determination of free amino acids content (GB/T 8314–2013)* (Standards Press of China, Beijing, 2013).
26. Yulong, Y. et al. Dynamic changes in amino acids, catechins, caffeine and gallic acid in green tea during withering. *J. Food Compos. Anal.* **66**, 98–108. <https://doi.org/10.1016/j.jfca.2017.12.008> (2018).
27. Juhua, Z. et al. Evaluation of astringent taste of green tea through mass spectrometry-based targeted metabolic profiling of polyphenols. *Food Chem.* **305**, 125507–125512. <https://doi.org/10.1016/j.foodchem.2019.125507> (2020).
28. Cesarettin, A. et al. Flavor characteristics of seven grades of black tea produced in Turkey. *J. Agric. Food Chem.* **60**, 6323–6332. <https://doi.org/10.1021/jf301498p> (2012).
29. Xia, Y. et al. Study on the chemical constituents of Hunan black tea. *J. Tea Sci.* **39**, 150–158. <https://doi.org/10.13305/j.cnki.jts.2019.02.004> (2019).
30. Peigen, Y., Angelinsoolee, Y., Meiyin, L. & Weibiao, Z. Identifying key non-volatile compounds in ready-to-drink green tea and their impact on taste profile. *Food Chem.* **155**, 9–16. <https://doi.org/10.1016/j.foodchem.2014.01.046> (2014).
31. Hua, S. et al. Caffeine excites medial parabrachial nucleus neurons of mice by blocking Adenosine A1 receptor. *Brain Res.* **1790**, 147984–147984. <https://doi.org/10.1016/j.brainres.2022.147984> (2022).
32. Yingna, Z. et al. Improving the sweet aftertaste of green tea infusion with tannase. *Food Chem.* **20**, 192–195. <https://doi.org/10.1016/j.foodchem.2015.07.046> (2016).
33. Ikotunabiodun, M., Ezugwuabsalom, E., Abualigah, L., Abuhaija, B. & Heming, J. K-means clustering algorithms: A comprehensive review, variants analysis, and advances in the era of big data. *Inf. Sci.* **622**, 178–210. <https://doi.org/10.1016/j.ins.2022.11.139> (2023).
34. Kanehisa, M., Furumichi, M., Sato, Y., Matsuura, Y. & Ishiguro-Watanabe, M. KEGG: Biological systems database as a model of the real world. *Nucleic Acids Res.* **53**, D672–D677. <https://doi.org/10.1093/nar/gkae909> (2025).
35. Hailing, H. et al. Metabolomics analysis reveals the effect of removing cotyledons on salt tolerance in castor plant roots during early seedling establishment. *Indus. Crops Prod.* **207**(P1), 117702. <https://doi.org/10.1016/j.indcrop.2023.117702> (2024).
36. Xiaona, Z., Chunlan, P., Youkui, D. & Minlong, C. Transcriptome analysis of response to heavy metal Cd stress in soybean root. *Chin. J. Appl. Ecol.* **28**, 1633–1641. <https://doi.org/10.13287/j.1001-9332.201705.004> (2017).
37. Adam C, E. et al. Sphingolipid metabolism drives mitochondria remodeling during aging and oxidative stress. *bioRxiv: the preprint server for biology*, 2025. <https://doi.org/10.1101/2025.02.26.640157> (2025).

Author contributions

J.Y., S.C., and L.Y. were pivotal in conceptualizing the research and overseeing its design. J.Y., S.C., J.W., and Y.Z. spearheaded the data analysis and interpretation. J.Y., S.C., R.C. and Y.Z. took responsibility for creating the figures and tables. J.Y., H.L. and S.C. drafted the initial version of the manuscript. L.Y., along with other contributors, reviewed and approved the final manuscript draft. L.Y. as the corresponding authors, ensured the integrity and accuracy of the work.

Funding

This work was supported by the Natural Science Foundation General Project of Chongqing (CSTB2022N-SCQ-MSX1668) and Chongqing Academy of Agricultural Sciences Municipal Financial Research Project (cq-as2023sjczqn015, KYLX20250600086).

Declarations

Competing interests

The authors declare no competing interests.

Ethics approval

This study was approved by the [Academic Committee of Chongqing Academy of Agricultural Sciences].

Additional information

Supplementary Information The online version contains supplementary material available at <https://doi.org/10.1038/s41598-026-39332-7>.

Correspondence and requests for materials should be addressed to L.Y.

Reprints and permissions information is available at www.nature.com/reprints.

Publisher's note Springer Nature remains neutral with regard to jurisdictional claims in published maps and institutional affiliations.

Open Access This article is licensed under a Creative Commons Attribution-NonCommercial-NoDerivatives 4.0 International License, which permits any non-commercial use, sharing, distribution and reproduction in any medium or format, as long as you give appropriate credit to the original author(s) and the source, provide a link to the Creative Commons licence, and indicate if you modified the licensed material. You do not have permission under this licence to share adapted material derived from this article or parts of it. The images or other third party material in this article are included in the article's Creative Commons licence, unless indicated otherwise in a credit line to the material. If material is not included in the article's Creative Commons licence and your intended use is not permitted by statutory regulation or exceeds the permitted use, you will need to obtain permission directly from the copyright holder. To view a copy of this licence, visit <http://creativecommons.org/licenses/by-nc-nd/4.0/>.

© The Author(s) 2026